HHS Public Access

Author manuscript

J Reprod Immunol. Author manuscript; available in PMC 2022 June 01.

Published in final edited form as:

J Reprod Immunol. 2021 June ; 145: 103309. doi:10.1016/j.jri.2021.103309.

Epithelial membrane protein 2 (*Emp2*) modulates innate immune cell population recruitment at the maternal-fetal interface

Alison Chu[a], **Su-Yin Kok**[b], **Jessica Tsui**[b], **Meng-Chin Lin**[a], **Brian Aguirre**[b], **Madhuri Wadehra**[b,‡,*]

[a]Division of Neonatology and Developmental Biology, Department of Pediatrics, David Geffen School of Medicine, University of California-Los Angeles, 10833 Le Conte Avenue, MDCC B2-411, Los Angeles, CA 90095 U.S.A;

[b]Department of Pathology, David Geffen School of Medicine, University of California-Los Angeles, 4525 MacDonald Research Laboratories, Los Angeles, CA 90095 U.S.A;

[‡]Jonsson Comprehensive Cancer Center, David Geffen School of Medicine at UCLA, David Geffen School of Medicine, University of California-Los Angeles, 4525 MacDonald Research Laboratories, Los Angeles, CA 90095 U.S.A;

Abstract

Epithelial membrane protein 2 (EMP2) is a tetraspan membrane protein that has been revealed in cancer and placental models to mediate a number of vascular responses. Recently, *Emp2* modulation has been shown to have an immunologic effect on uterine NK cell recruitment in the mouse placenta. Given the importance of immune cell populations on both placental vascularization and maternal immune tolerance of the developing fetus, we wanted to better characterize the immunologic effects of *Emp2* at the placental-fetal interface. We performed flow cytometry of WT and *Emp2* KO C57Bl/6 mouse uterine horns at GD12.5 to characterize immune cell populations localized to the various components of the maternal-fetal interface. We found that *Emp2* KO decidua and placenta showed an elevated overall percentage of CD45+ cells compared to WT. Characterization of CD45+ cells in the decidua of *Emp2* KO dams revealed an increase in NK cells, whereas in the placenta, *Emp2* KO dams showed an increased percentage of M1 macrophages (with an increased ratio of M1/M2 macrophages). Given the differences detected in uNK cell populations in the decidua, we further characterized the interaction between *Emp2* genetic KO and NK cell deletion via anti-asialo GM1 antibody injections. While the double knock-out of *Emp2* and NK cells did not alter individual pup birthweight, it significantly reduced total litter weight and size by ~50%. In conclusion, *Emp2* appears to regulate uNK and macrophage cell populations in pregnancy.

[*]Corresponding Author: Madhuri Wadehra, Pathology and Laboratory Medicine, 4525 MacDonald Research Laboratories, Geffen School of Medicine at UCLA, Los Angeles, CA 90095. Phone: (+1)-310-825-1590; Fax: (+1)-310-825-5674; mwadehra@mednet.ucla.edu.

Declarations of interest: M.W. is an inventor on the University of California patents related to anti-EMP2 monoclonal antibodies. M.W. was a consultant for OncoResponse, Inc. Seattle, WA.

Keywords

placenta; uterine natural killer cells; macrophages; epithelial membrane protein 2

1. Introduction

During pregnancy, the placental bed consists of many populations of immune cells. Within early pregnancy, 30–40% of all cells in the decidua are leukocytes(Bulmer, 1992, Harris et al., 2019) consisting of uterine Natural Killer (uNK) cells, macrophages and T lymphocytes(Kwan et al., 2014). Of these three populations, uNK cells and macrophages dominate, with the highest numbers observed during the first and second trimesters compared to the third trimester(Williams et al., 2009).

Natural Killer (NK) cells are innate lymphoid cell members that are derived from bone marrow-derived CD34+ hematopoietic progenitor cells and circulate in the blood(Sojka et al., 2019, Gaynor and Colucci, 2017). Within the non-gravid endometrium, uNK cells exist and expand during the secretory phase dominated by progesterone. In pregnancy, these cells represent the most abundant leukocytes in the uterus and within the maternal-fetal interface. While the exact function of uNK cells remains unclear, these cells have been well described as mediating trophoblast invasion and early spiral artery remodeling in the placenta(Faas and de Vos, 2017, Faas and De Vos, 2018).

Recently, epithelial membrane protein 2 (EMP2), a tetraspan membrane protein, was shown to regulate uNK cell recruitment during pregnancy(Williams et al., 2017). EMP2 has largely been described in cancer models and purported to have various functions involving cell adhesion, invasion and in the regulation of neoangiogenesis(Sun et al., 2019, Gordon et al., 2013, Patel et al., 2020). In mouse reproduction, *Emp2* is expressed in trophoblast cells throughout pregnancy, and knock-out of *Emp2* impairs early implantation(Wadehra et al., 2006) as well as placental angiogenesis(Williams et al., 2017) through modulation of VEGF and HIF1α. Interestingly, in the later study, we found that trophoblast-mediated uNK cell recruitment increased in *Emp2* knock-out (KO) animals in the placenta and persisted longer through gestation as compared to WT controls(Williams et al., 2017).

Given the unexpected effect of *Emp2* KO on immune cell populations in the placenta, we hypothesized that uNK cell recruitment during pregnancy is regulated in part by *Emp2* expression. In this study, we examined the effects of *Emp2* modulation on the dominant leukocyte populations found at the maternal-fetal interface, as the maintenance of the normal immunologic milieu affects pregnancy and fetal outcomes(Toth et al., 2020, Liu et al., 2017, Areia et al., 2019, Geldenhuys et al., 2018). We show that *Emp2* and NK cells work synergistically to regulate pregnancy outcomes.

2. Materials and Methods

2.1 Ethical Approval

This study was conducted in accordance with established guidelines in accordance with the NIH guide for the care and use of laboratory animals, and all protocols were approved by the

Animal Research Committee of the University of California Los Angeles in accordance with the guidelines set by the National Institutes of Health. *Emp2* KO C57BL/6 mice originally created in the laboratory of Dr. Carmen Williams (National Institute of Environmental Health Sciences (NIEHS) at the NIH) were re-derived at UCLA (Williams et al., 2017). These KO animals along with WT C57BL/6 mice obtained from the UCLA Division of Laboratory and Animal Medicine colony were housed in 12:12 hour light-dark cycles with *ad libitum* access to a standard rodent chow diet (Pico Lab Rodent Diet 20, cat# 5053, Lab Diet, St. Louis, MO) and water. At the end of the experimental period, mice underwent brief anesthesia using inhaled isofluorane (2–3 minutes) followed by cervical dislocation. The tissues of interest were dissected within 5 minutes of death, and immediately stored for downstream processing (either processed fresh for flow cytometry, or stored in formalin). All efforts were made to reduce the number of animals used for experiments and to minimize animal suffering.

Wild type and *Emp2* KO female mice were mated overnight with age-matched and strain-matched males. The morning after mating, plugged females were designated as pregnant at GD0.5. Pregnant females were housed singly, with *ad libitum* access to a standard rodent chow diet, as above. The WT vs KO status of animals was validated by western blot analysis as previously described using lung tissue (Williams et al., 2017) (Fig. S1).

2.2 Tissue Collection

After euthanasia, the abdominal cavity was opened for each pregnant mouse at GD12–13 (n=10–13 litters/group). Leukocyte isolation was performed as published in the literature(Arenas-Hernandez et al., 2015). Briefly, the uterine horn was removed by dissection at the uterotubal junctions, mesentery and cervix. The uterine horn size was recorded and then placed into PBS to keep the tissue hydrated. Sacs were separated by dissection at inter-implantation sites. On clear petri dishes, the uterine horn was opened by cutting the uterine wall open from each open end of the sac. The uterine myometrial tissue was removed, the decidua dissected from the fetal placenta, and the placenta separated from the fetus and chorioallantoic membrane. Each fetus and placenta were weighed separately and dissociated both enzymatically and mechanically as described below

2.3 Tissue Dissociation and Leukocyte Purification

For each pregnant dam, 2–3 placentas and deciduas were pooled, and all tissues were kept on ice. 100–150 mg of uterine myometrial, placental, or decidual tissue were transferred to tubes containing 500 μl cold Accutase reagent (Life Technologies #A11105–01). Tissues were minced using sterile scissors for no more than 2 minutes after which another 500 μl of cold Accutase reagent were added. Samples were then incubated horizontally in a 37° incubator for 30–35 minutes while shaking at 80 rpm. Tubes were then placed on ice to prevent further digestion and then poured through a 70 μm strainer into 50 ml tubes. 50ml tubes were centrifuged at 1250 g for 10 minutes at 4°C. Supernatants were aspirated, and then the pellet was resuspended in 1 ml RPMI without FBS. 500 μl of neat FBS was added to a 5 ml polystyrene plastic tube, and the cell suspension was slowly overlaid on top of FBS. The samples were then centrifuged at 1100 g for 10 minutes at 20°C without brake.

Cells were washed and diluted to a final concentration of 10×10^6 cells/ml in FACS buffer (0.5% BSA + 0.05% NaN_3 in PBS buffer).

2.4 Flow staining

For each sample, 100 μl of 10×10^6 cells/ml were transferred into a 96-well plate. Cells were resuspended in 1:1000 dilution of LIVE/DEAD® Fix-able Dead Cell Stain kit (Invitrogen #L34962) for 30 minutes at 4°C in darkness. Cells were treated with mouse Fc block (anti-CD16/32 (BioLegend #101302) and stained for surface markers. Cells were treated with the following antibody mix in FACS buffer: anti-F4/80-PerCP-Cy5.5 (clone: BM8; eBioscience), anti-CD25-BV421 (clone: PC61.5; eBioscience), anti-FR4 PE-Cy7 (clone: 12A5; BioLegend), anti-CD49b PE-Dazzle594 (clone: DX5; BioLegend), anti-CD3ε-BV785 (clone: 145–2C11; BioLegend), anti-CD4 eFluor650 (clone: GK1.5; eBioscience), anti-CD206 BV605 (clone: C068C2; BioLegend), anti-MHCII AlexaFluor700 (clone: M5/114.15.2; eBioscience), and anti-CD45.2 APC (clone: 104; eBioscience). Cells were incubated for 30 minutes, washed, and then resuspended in 300 μl of FACS buffer. Samples were analyzed on the LSRII machine within the UCLA Flow Cytometry Core.

UltraComp™ eBeads were purchased from eBioscience and used for compensation. Live cells were gated based on forward- and side-scatter properties and the absence of fluorescence based on the LIVE/DEAD staining. Samples analyzed had >85% viability, and 100,000 live cells were acquired per tube. Flow cytometry analysis was performed using FlowJo software version 10 (BD Biosciences, Ashland, Oregon).

All gating was performed based on live cell populations. Unstained controls and single color controls (uteri and spleen) were utilized to establish base line gate settings for each respective anti-flurophore combination used in individual experiments. Manual compensation was used, as it allowed for an optimal adjustment of the spectral overlap between the different fluorochromes. The gating strategy for each cell-type examined is outlined below, based on previous works(Hensel et al., 2019, Au - Monaghan et al., 2020) and can be visualized in Supplementary Fig. 2.

CD4+ T cells P1 = live cells, P2 = CD45 positive gate, P3 = CD3ε and CD4 double positive gate

CD4+ T regs P1 = live cells, P2 = CD45 positive gate, P3 = CD3ε and CD4 double positive gate, P4 = CD25 and FR4 double positive cells

CD8+ T cells P1 = live cells, P2 = CD45 positive gate, P3 = CD3ε positive and CD4 negative cells

Macrophages P1 = live cells, P2 = CD45 positive gate, P3 = F/480 positive and CD4 negative cells

M1 Macrophages P1 = live cells, P2 = CD45 positive gate, P3 = F/480 positive and CD4 negative cells, P4 = MHC II positive cells and CD206 negative cells

M2 Macrophages P1 = live cells, P2 = CD45 positive gate, P3 = F/480 positive and CD4 negative cells, P4 = CD206 positive cells and MHC II negative cells

NK cells P1 = live cells, P2 = CD45 positive gate, P3 = CD49b positive and MHC II negative cells

2.5 Histology and Immunohistochemistry

In some experiments, after harvesting, tissues of interest (uterine horns, placentas, spleen) were rinsed in PBS, fixed in cold 10% neutral buffered formalin for 24 hours, and then transferred to 70% ethanol. Samples were embedded in paraffin, sectioned at 5 μm and stained with hematoxylin and eosin by the Translational Pathology Core Laboratory (TPCL) at UCLA. Other sections were stained by immunohistochemistry for NK cells as previously described(Chu et al., 2016). Briefly, samples were deparaffinized and dehydrated in alcohol. Antigen retrieval was performed using 0.1mol/L citrate, pH 6.0, at 95°C for 20 minutes. Uterine NK cells were assessed using biotinylated Dolichos Biflorus Agglutinin (DBA) -Lectin (Zhang et al., 2009) (1:500; Vector labs) followed by Streptavidin-HRP per manufacturer's instructions (Vector Labs, PK6101; Burlingame, CA). NK cells were identified using a DAB substrate as previously described (Williams et al., 2017).

M1 and M2 macrophages were identified using antibodies. Formalin-fixed paraffin-embedded samples were deparaffinized as above, and following antigen retrieval, the slides were put into 3% H_2O_2 in 70% methanol for 30 minutes to block endogenous peroxidase activity. Next an ImmEdge pen (#H-4000, Vector Laboratories, Burlingame, CA) was used to create a hydrophobic barrier for each section. 100–200 μl of TrueBlack Lipofuscin Autofluorescence Quencher (1X in 70% ethanol, #23007, Biotium, Fremont, CA) was applied to each section for 30 seconds to 1 minute to quench autofluorescence. Immediately after 3 times of PBS wash, horse serum (2.5% in PBS) as blocking solution was placed on the tissues for 30 minutes at room temperature in a moist container. Then the primary antibodies at 1:100 dilution in PBS were applied onto each section overnight at 4°C (M1: iNOS, monoclonal mouse IgG, #MAB9502, R&D Systems, Minneapolis, MN; M2: CD206, polyclonal goat IgG, #AF2535, R&D Systems, Minneapolis, MN). Some sections were incubated with isotype negative control antibodies including monoclonal mouse IgG1and polyclonal goat IgG from R&D Systems (#MAB002 and #AB-108-C, respectively). After three times of 5-minute washes in PBS, the secondary antibodies (for M1, donkey anti-mouse 594, #A32744, Invitrogen, Carlsbad, CA; for M2, rabbit anti-goat 488, #A-11078, Invitrogen, Carlsbad, CA) at 1:200 concentration diluted in PBS were applied to the sections for 60 minutes in the dark. Following another three times of 5-minute washes in PBS, 100–200 ml of 4',6-diamidino-2-phenylindole (DAPI for nuclear staining, 1:30,000, #D21490, Invitrogen, Carlsbad, CA) was applied for 5 minutes in the dark. The slides were rinsed in ddH_2O, and then mounted using ProLong (#P10144, ThermoScientific, Waltham, MA). Staining was evaluated and quantified using a 10x objective on a fluorescent Olympus BX-51 (Waltham, MA) microscope.

To perform area analysis, unmodified, uncompressed .tif image files of the placenta were accessed using Adobe Photoshop CS5 (Version 12.0.4). The pixel numbers for NK cell staining were obtained using the histogram window and the magic wand to select all positive

cells (Window > Histogram > Expanded view > Pixel number). In order to assess M1 and M2 macrophage staining, an optical density plot of the selected area was generated using the Histogram tool in the Image menu. The mean staining intensity in the red channel (M1 macrophages) or green channel (M2 macrophages) was recorded for each group. Background staining was determined using slides stained with the isotype control. Immunostaining intensity was calculated as the difference between mean immunostaining for each color and background immunostaining as previously described(Lehr et al., 1997, Agley et al., 2012).

2.6 Western blot analysis

Mouse tissues were processed using fresh specimens and immediately frozen on dry ice. Tissues were homogenized using a glass-Teflon homogenizer and tissue was immediately placed in cold Laemmli buffer containing protease and phosphatase inhibitors (Millipore Sigma, St. Louis, MO). EMP2 expression was detected by treating cell extracts with peptide N-glycosidase F (New England Biolabs, Beverly, MA, USA). Lysates were then separated on a Tris-Glycine polyacrylamide gel (Thermo-Fisher Scientific, Waltham, MA), and proteins were transferred onto nitrocellulose. EMP2 was detected using rabbit anti-mouse EMP2(Fu et al., 2013) (1:1000) antiserum followed by a HRP-conjugated goat anti-rabbit IgG and Luminata Crescendo chemiluminescence detection reagents (Millipore Sigma).

2.7 Anti-asialo GM1 injections

Pregnant females were singly housed and received intraperitoneal (IP) injections of 100 μl of anti-asialo GM1 antisera (Wako, Richmond, VA, cat #986–10001) or sham (matched host rabbit polyclonal IgG; BioXcell, cat#BE0095) at GD4, 6.5, and 9, as published for systemic NK cell depletion in pregnancy(Freitag et al., 2014, Tirado-González et al., 2012, Murphy et al., 2005). This resulted in four experimental conditions: WT + sham (WT), WT + anti-asialo GM1 (NK KO), *Emp2* KO + sham (*Emp2* KO), and *Emp2* KO + anti-asialo GM1 (*Emp2* DKO).

In some females (n=6/group), uterine horns and spleens were collected at GD12–13 to confirm NK depletion as well as immune cell recruitment. Others were allowed to carry their fetuses to term and to deliver their pups (n=18–24 pups/group from 3–4 litters/group). Pup weights were taken at birth and litters counted. Total litter weight was calculated by adding the birth weights of all pups within a single litter.

2.8 Statistical Analysis

All statistical analyses described were conducted in GraphPad Prism software (version 5, GraphPad Software Inc., La Jolla, CA), and normal distribution was tested for using the data obtained from both groups using the Shapiro-Wilk normality test. Data is presented as means ± SEM when data demonstrates normal distribution, and as median and quartile range when data did not demonstrate normal distribution, unless otherwise indicated. To test for significant differences between two groups (WT and *Emp2* KO) data with normal distribution (e.g. specific immune cell populations in specific tissues), we analyzed results using the Student's t-test for parametric data. To compare data that did not demonstrate normal distribution (e.g. specific immune cell populations in specific

tissues), Mann-Whitney U testing was used. When multiple groups were compared and data demonstrated normal distribution, ANOVA testing was used (e.g. pup birth weights); when data did not demonstrate normal distribution, Kruskal-Wallis testing was performed. All p-values are reported as 2-tailed with statistical significance set at <0.05 for all comparisons. Sample sizes were determined by power calculations with a power of 0.8, type I error rate of 5%, to detect a 25% difference in the percentage of total immune cells with a standard deviation of 2%, requiring a sample size of 3 samples/group.

3. Results

3.1 Immunophenotyping of the tissues at the maternal-fetal interface

Outside of the presence of uNK cells, little is known about the regulation of immune cells by *Emp2* at the maternal-fetal interface. In order to compare the *Emp2* KO with control C57B/6, pregnant animals at GD12.5 were isolated with individual sites corresponding to the uterus, decidua and placenta obtained. Fig. S1 confirmed *Emp2* levels in the WT and KO animals using lung tissue. GD12.5 was selected as, by this time point, the chorioallantoic placenta was established, and it loosely represents a late first trimester time point in humans(Ander et al., 2019). In both groups, the percentage of CD45+ cells was highest in the decidua, followed by the placenta and uterus (Fig. 1A). The percentage of CD45+ immune cells of all live cells was increased in the *Emp2* KO mice compared to the WT mice in the decidua (p=0.045) and the placenta (p=0.034), but not in the uterus (p=0.07; Fig. 1B).

We next examined specific cell populations as a percentage of total CD45+ cells at distinct locations within the placental bed, specifically examining the percentage of T cells, uNK cells, and macrophages. Fig. S2 details the analytical template for immune populations. With regard to T cells, no differences were observed in the percentage of CD3+ cells between both sets of animals (Fig. 2A). When CD3+ cells were dichotomized using CD4 expression, there was roughly a 3:1 ratio of CD4− (classified as CD8+ by default) to CD4+ cells (Fig. 2B, Fig. 2C, respectively). No differences were observed between sites for CD8+ or CD4+ cells in dams from both sets of animals.

To further investigate if differences existed in CD4+ subpopulations, cells were further interrogated based on CD25 and Folate Receptor 4 (FR4) expression to identify regulatory T cells (Tregs)(Kurniawan et al., 2020, Jørgensen et al., 2019). Tregs mediate self-tolerance as well as play an essential role in the suppression of immune responses, and in pregnancy, low numbers of Tregs correlate with complications such as preeclampsia and pregnancy failure(Tsuda et al., 2019). Of the CD4+ cells found along the uterus, decidua, and placenta, approximately 30% were Treg cells although the absolute numbers of these cells were small (Fig. 2C, right and Fig. S2). Significantly, higher numbers of Tregs occurred in the decidua and placenta of WT animals compared to the *Emp2* KO, suggesting that these cells may play a protective role in WT pregnancies (p=0.02, p=0.04, respectively).

uNK cells, in contrast to T cells, were more abundant throughout the maternal-fetal interface. uNK cells were significantly enriched in the decidua of *Emp2* KO dams compared to the uterus and placenta (p=0.021) whereas there were no significant differences in the uNK distribution across tissues in WT mice (Fig. 2B). Similarly, a statistically significant

increase in the percentage of uNK cells (relative to CD45 levels) was observed in *Emp2* KO decidua compared to WT decidua (p=0.023; Fig. 2B), corresponding to an ~40% (27.1±2.8) increase in uNK cells observed in *Emp2* KO compared to WT decidua (19.5±1.7).

In both groups of animals, macrophages represented a significant number of CD45+ immune cells isolated in all locations at GD12.5 (decidua, placenta, and uterus). While uNK cells were most abundant within the decidua, macrophages were the most prevalent leukocytes within the uterus and placenta. The distribution differences in the percentage of macrophages across the three tissues were significant in WT mice, (highest percentage in placenta and lowest in decidua; p=0.029), whereas no statistical differences in distribution occurred in *Emp2* KO tissues (Fig. 3A). When WT and *Emp2* KO groups were directly compared, the percentage of all macrophages (F4/80+) relative to the CD45+ cell population were not statistically different within the uterus, decidua or placenta (Fig. 3A).

Macrophages exist as heterogenous populations throughout tissue(Mezouar et al., 2020) and are typically described by their activation and polarization state. M1 macrophages typically have a pro-inflammatory signature and produce NO, while M2 macrophages promote cell proliferation and tissue repair(Orecchioni et al., 2019). When considering M1 macrophages (MHCII+) relative to all macrophages (F4/80+), there was a significant increase in the percentage of M1 macrophages in *Emp2* KO placenta compared to WT placenta (p=0.027; Fig. 3B). In contrast, M2 macrophages characterized as CD206+/MHCII^{low}, displayed a similar distribution across tissue types in both WT and *Emp2* KO groups (Fig. 3C). When examining the ratio of M1/M2 macrophages within the placenta, a statistically significantly increase occurred in the *Emp2* KO placenta compared to the WT placenta (p=0.032; Fig. 3D).

3.2 NK cell depletion in pregnancy

We have previously reported that *Emp2* is expressed in secretory endometrium as well as multiple trophoblast lineages including extravillous trophoblasts where it is believed to help regulate invasion and neoangiogenesis(Williams et al., 2017). Given the increase in uNK cells observed in the *Emp2* KO animals, we hypothesized that an interplay between uNK cells and trophoblasts may exist mediated in part by *Emp2*. In the absence of *Emp2*, we speculated that uNK cells may provide a compensatory response to improve trophoblast invasion and spiral artery remodeling. To test this theory, systemic NK cell depletion was undertaken with gestational anti-asialo GM1 injections. Uterine NK cell depletion was verified by DBA-lectin staining of the spleen and placenta after IP injections of anti-asialo GM1 antibody as described above (Fig. 4A, Fig. S3, respectively). Interestingly, depletion of NK cells alone did not affect litter weight, litter size or individual pup birthweight. However, there was a significant reduction in total litter weight in the *Emp2* double KO (DKO) group compared to the WT, NK KO, and *Emp2* KO groups (p=0.02 by Kruskal-Wallis testing) (Fig. 4B). This difference was attributable to a reduction in the litter size (number of pups) in the *Emp2* DKO group (p=0.0094) and not to the birthweight of the pups (p=0.9218) (Fig. 4C–D). When we evaluated the uterine horns at GD12.5, we observed that *Emp2* DKO results in increased resorption of the fetus within individual sacs supporting the idea that EMP2 and uNK cells regulate early pregnancy establishment.

3.3 Alterations in Macrophage Localization

Macrophages are induced along M1 or M2 phenotypes throughout pregnancy. A tightly regulated and dynamic process, inappropriate macrophage polarization correlates with abnormal outcomes, and it has been implicated in inducing spontaneous abortions, preterm labor, and preeclampsia(Yao et al., 2019, Faas et al., 2014). As flow cytometric characterization of the *Emp2* KO placentas suggested an increase in M1 polarization, we investigated the localization of M1 and M2 decidual macrophages at GD12.5.

Similar to flow cytometric analysis, using immunohistochemical staining, we observed an increase in M1 and M2 macrophages populations throughout the decidua of the *Emp2* KO animals compared to the WT (Fig. 5A). M1 and M2 macrophage subsets were identified through differences in metabolic signaling using iNOS or arginase staining, respectively(Yao et al., 2019). Comparisons of the DKO with the WT sham-treated animals revealed an increase in M1 and M2 macrophages in the deciduas of the DKO placentas (Fig. 5B; Fig. S4). M1 macrophages showed significant differences between groups (ANOVA, $p=0.01$), with the number of M1 macrophages trending higher in the DKO compared to the single KO animals. Similarly, analysis of the M2 macrophages revealed significant differences among the groups (ANOVA, $p=0.02$), with the highest levels observed in the DKO. These results collectively suggest that modification of Emp2 and NK cells increase recruitment of macrophages into the decidua and suggest a mechanism by which pregnancy loss occurred.

4. Discussion

In both human and animal models, several studies have shown that uNK cells and macrophages represent the main immune cell populations present at the maternal-fetal interface (Faas and De Vos, 2018, Faas and de Vos, 2017). These immune cells are essential for survival of the fetus by maintaining fetal tolerance during pregnancy, but they also mediate a number of essential processes that ensure adequate fetal growth such as early vascular remodeling at the maternal-fetal interface(Negishi et al., 2018). For example, uNK cells have been described to contribute to spiral artery remodeling in vitro utilizing human decidual and endometrial samples (Lash et al., 2006, Li et al., 2001). Given that previously published studies on the role of *Emp2* in pregnancy suggest that uNK cell populations are both increased and persistent over gestation in *Emp2* KO mice compared to WT C57BL/6J mice(Williams et al., 2017), we conducted this study to specifically query whether uNK cells provide a compensatory mechanism to allow for early pregnancy establishment.

Consistent with our previous study, we found that uNK cells are increased in *Emp2* KO mice during pregnancy. This effect was refined in this study, showing that this effect is significant only in the decidua, not in the placenta or uterus. In one meta-analysis of studies comparing fertile to infertile human women, altered uNK cell amount was associated with adverse pregnancy outcomes such as recurrent pregnancy loss(Seshadri and Sunkara, 2014), a condition that may be associated with placental insufficiency.

In murine pregnancies, previous studies have shown that uNK cells make up a large percentage of leukocytes within the decidua(Sojka et al., 2019, Faas and de Vos, 2017), and this is consistent with the results presented here. The source of uNK cells remains

contested, with some suggesting that accumulation of cells early in pregnancy originates from local proliferating tissue resident NK cells while others suggest that peripheral NK cells are actively recruited from circulation(Sojka et al., 2018, Doisne et al., 2015). NK cells were originally recognized for their recognition of and cytotoxicity against virally-infected or neoplastic host cells. Advances in NK cell biology have uncovered alternate functional NK cell states in mice and in humans, some proficient for cytotoxicity, but others predominantly devoted to cytokine production and its regulatory impact on local tissue function (Kadri et al., 2015, Fauriat et al., 2010, Anfossi et al., 2006, Horowitz et al., 2016). In the placenta, uNK cells do not exhibit cytotoxic activity, but instead, they produce factors which are believed to help regulate trophoblast function and arterial remodeling. Previous studies have shown that uNK cell functions are regulated, in part, by direct contact between uNK cells and trophoblasts as NK cell receptors are known to bind unique forms of HLA molecules on extravillous trophoblasts(King et al., 2000). Interestingly, *Emp2* expression in vitro strongly augments levels of MHC1 proteins in murine cell lines (Wadehra et al., 2003), and it is possible that alterations of these levels may modulate the cytokine profile of uNK cells. In humans, the interactions between NK cell killer Ig-like receptors and MHC-I ligands in specific maternal-fetal combinations have been associated with preeclampsia. Mice interestingly display decidual vessel, placental size, and fetal weight differences that are dependent upon specific combinations of maternal-fetal MHC-1 haplotypes, suggesting that, in spite of the known differences between mouse and human pregnancy states, murine pregnancy is a feasible model to study NK cell interactions (Wu et al., 2013, Madeja et al., 2011, Kieckbusch et al., 2014). Indeed, studies by Croy et al utilizing genetic mouse models to target specific components of NK cell interaction, such as Ly49 receptors (the mouse equivalent of human KIRs), aryl hydrocarbon receptor (AHR) and natural cytotoxicity receptors (NCR), support important roles for these receptors in promoting normal physiologic pregnancy in mice(Felker et al., 2013, Leon et al., 2016, Felker and Croy, 2017).

We undertook systemic NK cell depletion to better understand the biologic effects of NK cell depletion in the setting of *Emp2* genetic knock-out. Depletion of NK cells using anti-asialo GM1 injections had no impact on fetal weight and litter size in WT mice, and this effect is consistent with other studies using these agents in rats(Golic et al., 2016). However, when these injections were performed in *Emp2* KO animals, histologic examination at GD12.5 showed evidence of resorption of 50% of individual implantation sites in the *Emp2* DKO with 50% developing normally in WT dams. This dichotomy is interesting and suggests that, in fact, early NK cell depletion in combination with *Emp2* KO leads to implantation defects or resorption of the fetus.

We also found that *Emp2* KO mice demonstrate an increase in M1-type macrophages in the decidua, compared to WT mice. Macrophages play an important role in healthy human pregnancy. At the maternal-fetal interface, both the number and proportion of M1/M2 macrophages purportedly change during gestation to allow for spiral artery remodeling and protect the fetus from the maternal immune microenvironment and establish fetal-maternal tolerance(Yao et al., 2019). Classically, macrophages have been described in subsets, with skewing towards an M1 (classically activated) phenotype or M2 (alternatively activated) phenotype, and it has been shown that an appropriate M1/M2 balance is necessary for

the establishment and maintenance of a normal pregnancy(Zhang et al., 2017). Indeed, the skewing towards M1-type macrophages at GD12.5 in the decidua may be contributing towards the later phenotype of "placental insufficiency" seen in *Emp2* KO mice(Williams et al., 2017), and it is intriguing to speculate that the relative skewing towards M1 phenotype macrophages in our *Emp2* KO may contribute to a local pro-inflammatory milieu and fetal loss at individual implantation sites.

In line with this hypothesis, DKO animals showed increased numbers of M1 and M2 macrophages. It has been suggested that after trophoblasts invade the endometrium, decidual macrophages begin to transform to mixed M1/M2 profiles(Yao et al., 2019), but in our experiments no colocalization in iNOS and CD206 staining was observed. Examining each population individually, previous studies in humans suggest that high numbers of decidual M1-like macrophages correlate with spontaneous preterm labor patients (needs ref), and in our experiments, *Emp2* and NK DKO animals demonstrated increased numbers of this subset. In healthy pregnancy, after placentation is complete, macrophages shift toward M2 polarization until parturition and contribute to tissue repair, angiogenesis, and immunomodulation. While future experiments will be needed to determine the timing for the influx of cells into the placenta, the high M1 and M2 numbers suggest that NK cells depletion coupled with a loss of EMP2 synergistically work to recruit more macrophages into the placenta. It may be, as suggested by others(Bonney and Johnson, 2019, Yao et al., 2019), that the high numbers of macrophages simply reflect the stress within the placenta from loss of NK cells and *Emp2*.

In addition to uNK and macrophages, a dysregulation in the percentage of CD4+ Tregs was observed between the *Emp2* and WT dams. In pregnancy, CD4+ Tregs help maintain an active state of maternal immune tolerance as they contain inflammation, inhibit adaptive immunity and support maternal vascular adaptations, and in this way, they help regulate trophoblast invasion and placental access to the maternal blood supply(Robertson et al., 2018, Svensson-Arvelund et al., 2015). Curiously, no significant changes were observed in the percentage of CD4+ and CD8+ T cells, and it is of note that the total numbers of Tregs observed were small. Thus, additional experiments will be needed to determine if Emp2 plays a substantial role in the regulation of these cells.

Prior to this study, there have been very few studies on how *Emp2* may modulate immune cell recruitment in tissues. One recent study in murine lung utilizing *Emp2* KO mice demonstrates that *Emp2* governs transepithelial migration of neutrophils (PMID 31550239) and it may be that at the maternal-fetal interface, *Emp2* acts similarly to regulate leukocyte recruitment to the decidua. Given that our study demonstrates that *Emp2* genetic knock-out leads to an alteration in the two main immune cell populations at the maternal fetal interface, we believe that *Emp2* modulates a maternal immune response along the sterile inflammation spectrum, which disrupts key mechanisms of pregnancy maintenance. Further interrogation, including comprehensive stereological assessment of the different compartments of the implantation site, will elucidate the cross-talk between trophoblasts and immune cell populations, and may reveal a role for targeting of *Emp2* to modify the M1/M2 balance and disordered NK cell recruitment that contribute towards adverse pregnancy outcomes.

Supplementary Material

Refer to Web version on PubMed Central for supplementary material.

Acknowledgements:

We thank Carmen Williams (NIEHS) for help with the rederivation of the *Emp2* KO colony.

Funding:

This work was generously supported by the National Institutes of Health NICHD K08-HD093874-03 (A.C.) and NCI R01 CA163971 (M.W.).

References

Agley CC, Velloso CP, Lazarus NR & Harridge SDR 2012. An image analysis method for the precise selection and quantitation of fluorescently labeled cellular constituents: application to the measurement of human muscle cells in culture. The journal of histochemistry and cytochemistry : official journal of the Histochemistry Society, 60, 428–438. [PubMed: 22511600]

Ander SE, Diamond MS & Coyne CB 2019. Immune responses at the maternal-fetal interface. Sci Immunol, 4.

Anfossi N, André P, Guia S, Falk CS, Roetynck S, Stewart CA, Breso V, Frassati C, Reviron D, Middleton D, Romagné F, Ugolini S & Vivier E 2006. Human NK cell education by inhibitory receptors for MHC class I. Immunity, 25, 331–42. [PubMed: 16901727]

Areia AL, Moura P, Mota-Pinto A & Crd42018089859 PN 2019. The role of innate immunity in spontaneous preterm labor: A systematic review. J Reprod Immunol, 136, 102616. [PubMed: 31581042]

Arenas-Hernandez M, Sanchez-Rodriguez EN, Mial TN, Robertson SA & Gomez-Lopez N 2015. Isolation of Leukocytes from the Murine Tissues at the Maternal-Fetal Interface. J Vis Exp, e52866. [PubMed: 26067389]

Au - Monaghan KL, Au - Farris BY, Au - Zheng W & Au - Wan ECK 2020. Characterization of Immune Cells and Proinflammatory Mediators in the Pulmonary Environment. JoVE, e61359.

Bonney EA & Johnson MR 2019. The role of maternal T cell and macrophage activation in preterm birth: Cause or consequence? Placenta, 79, 53–61. [PubMed: 30929747]

Bulmer JN 1992. Immune aspects of pathology of the placental bed contributing to pregnancy pathology. Baillieres Clin Obstet Gynaecol, 6, 461–88. [PubMed: 1332834]

Chu A, Thamotharan S, Ganguly A, Wadehra M, Pellegrini M & Devaskar SU 2016. Gestational food restriction decreases placental interleukin-10 expression and markers of autophagy and endoplasmic reticulum stress in murine intrauterine growth restriction. Nutr Res, 36, 1055–1067. [PubMed: 27865347]

Doisne JM, Balmas E, Boulenouar S, Gaynor LM, Kieckbusch J, Gardner L, Hawkes DA, Barbara CF, Sharkey AM, Brady HJ, Brosens JJ, Moffett A & Colucci F 2015. Composition, Development, and Function of Uterine Innate Lymphoid Cells. J Immunol, 195, 3937–45. [PubMed: 26371244]

Faas MM & De Vos P 2017. Uterine NK cells and macrophages in pregnancy. Placenta, 56, 44–52. [PubMed: 28284455]

Faas MM & De Vos P 2018. Innate immune cells in the placental bed in healthy pregnancy and preeclampsia. Placenta, 69, 125–133. [PubMed: 29748088]

Faas MM, Spaans F & De Vos P 2014. Monocytes and Macrophages in Pregnancy and Pre-Eclampsia. Frontiers in Immunology, 5.

Fauriat C, Long EO, Ljunggren HG & Bryceson YT 2010. Regulation of human NK-cell cytokine and chemokine production by target cell recognition. Blood, 115, 2167–76. [PubMed: 19965656]

Felker AM, Chen Z, Foster WG & Croy BA 2013. Receptors for non-MHC ligands contribute to uterine natural killer cell activation during pregnancy in mice. Placenta, 34, 757–64. [PubMed: 23806179]

Felker AM & Croy BA 2017. Natural cytotoxicity receptor 1 in mouse uNK cell maturation and function. Mucosal Immunol, 10, 1122–1132. [PubMed: 28098245]

Freitag N, Zwier MV, Barrientos G, Tirado-Gonzalez I, Conrad ML, Rose M, Scherjon SA, Plosch T & Blois SM 2014. Influence of relative NK-DC abundance on placentation and its relation to epigenetic programming in the offspring. Cell Death Dis, 5, e1392. [PubMed: 25165878]

Fu M, Brewer S, Olafsen T, Wu AM, Gordon LK, Said J, Braun J & Wadehra M 2013. Positron emission tomography imaging of endometrial cancer using engineered anti-EMP2 antibody fragments. Mol Imaging Biol, 15, 68–78. [PubMed: 22585360]

Gaynor LM & Colucci F 2017. Uterine Natural Killer Cells: Functional Distinctions and Influence on Pregnancy in Humans and Mice. Front Immunol, 8, 467. [PubMed: 28484462]

Geldenhuys J, Rossouw TM, Lombaard HA, Ehlers MM & Kock MM 2018. Disruption in the Regulation of Immune Responses in the Placental Subtype of Preeclampsia. Front Immunol, 9, 1659. [PubMed: 30079067]

Golic M, Haase N, Herse F, Wehner A, Vercruysse L, Pijnenborg R, Balogh A, Saether PC, Dissen E, Luft FC, Przybyl L, Park JK, Alnaes-Katjavivi P, Staff AC, Verlohren S, Henrich W, Muller DN & Dechend R 2016. Natural Killer Cell Reduction and Uteroplacental Vasculopathy. Hypertension, 68, 964–73. [PubMed: 27550919]

Gordon LK, Kiyohara M, Fu M, Braun J, Dhawan P, Chan A, Goodglick L & Wadehra M 2013. EMP2 regulates angiogenesis in endometrial cancer cells through induction of VEGF. Oncogene, 32, 5369–5376. [PubMed: 23334331]

Harris LK, Benagiano M, D'elios MM, Brosens I & Benagiano G 2019. Placental bed research: II. Functional and immunological investigations of the placental bed. Am J Obstet Gynecol, 221, 457–469. [PubMed: 31288009]

Hensel JA, Khattar V, Ashton R & Ponnazhagan S 2019. Characterization of immune cell subtypes in three commonly used mouse strains reveals gender and strain-specific variations. Lab Invest, 99, 93–106. [PubMed: 30353130]

Horowitz A, Djaoud Z, Nemat-Gorgani N, Blokhuis J, Hilton HG, Béziat V, Malmberg KJ, Norman PJ, Guethlein LA & Parham P 2016. Class I HLA haplotypes form two schools that educate NK cells in different ways. Sci Immunol, 1.

Jørgensen N, Persson G & Hviid TVF 2019. The Tolerogenic Function of Regulatory T Cells in Pregnancy and Cancer. Frontiers in Immunology, 10.

Kadri N, Thanh TL & Höglund P 2015. Selection, tuning, and adaptation in mouse NK cell education. Immunol Rev, 267, 167–77. [PubMed: 26284477]

Kieckbusch J, Gaynor LM, Moffett A & Colucci F 2014. MHC-dependent inhibition of uterine NK cells impedes fetal growth and decidual vascular remodelling. Nat Commun, 5, 3359. [PubMed: 24577131]

King A, Hiby SE, Gardner L, Joseph S, Bowen JM, Verma S, Burrows TD & Loke YW 2000. Recognition of trophoblast HLA class I molecules by decidual NK cell receptors--a review. Placenta, 21 Suppl A, S81–5. [PubMed: 10831129]

Kurniawan H, Soriano-Baguet L & Brenner D 2020. Regulatory T cell metabolism at the intersection between autoimmune diseases and cancer. European Journal of Immunology, 50, 1626–1642. [PubMed: 33067808]

Kwan M, Hazan A, Zhang J, Jones RL, Harris LK, Whittle W, Keating S, Dunk CE & Lye SJ 2014. Dynamic changes in maternal decidual leukocyte populations from first to second trimester gestation. Placenta, 35, 1027–34. [PubMed: 25449030]

Lash GE, Schiessl B, Kirkley M, Innes BA, Cooper A, Searle RF, Robson SC & Bulmer JN 2006. Expression of angiogenic growth factors by uterine natural killer cells during early pregnancy. J Leukoc Biol, 80, 572–80. [PubMed: 16816146]

Lehr H-A, Mankoff DA, Corwin D, Santeusanio G & Gown AM 1997. Application of Photoshop-based Image Analysis to Quantification of Hormone Receptor Expression in Breast Cancer. Journal of Histochemistry & Cytochemistry, 45, 1559–1565. [PubMed: 9358857]

Leon L, Felker AM, Kay VR, Tu MM, Makrigiannis AP & Croy BA 2016. Ly49 knockdown in mice results in aberrant uterine crypt formation and impaired blastocyst implantation. Placenta, 39, 147–50. [PubMed: 26992687]

Li XF, Charnock-Jones DS, Zhang E, Hiby S, Malik S, Day K, Licence D, Bowen JM, Gardner L, King A, Loke YW & Smith SK 2001. Angiogenic growth factor messenger ribonucleic acids in uterine natural killer cells. J Clin Endocrinol Metab, 86, 1823–34. [PubMed: 11297624]

Liu S, Diao L, Huang C, Li Y, Zeng Y & Kwak-Kim JYH 2017. The role of decidual immune cells on human pregnancy. J Reprod Immunol, 124, 44–53. [PubMed: 29055791]

Madeja Z, Yadi H, Apps R, Boulenouar S, Roper SJ, Gardner L, Moffett A, Colucci F & Hemberger M 2011. Paternal MHC expression on mouse trophoblast affects uterine vascularization and fetal growth. Proceedings of the National Academy of Sciences of the United States of America, 108, 4012–4017. [PubMed: 21300875]

Mezouar S, Katsogiannou M, Ben Amara A, Bretelle F & Mege JL 2020. Placental macrophages: Origin, heterogeneity, function and role in pregnancy-associated infections. Placenta, 103, 94–103. [PubMed: 33120051]

Murphy SP, Fast LD, Hanna NN & Sharma S 2005. Uterine NK cells mediate inflammation-induced fetal demise in IL-10-null mice. J Immunol, 175, 4084–90. [PubMed: 16148158]

Negishi Y, Takahashi H, Kuwabara Y & Takeshita T 2018. Innate immune cells in reproduction. J Obstet Gynaecol Res, 44, 2025–2036. [PubMed: 30058156]

Orecchioni M, Ghosheh Y, Pramod AB & Ley K 2019. Macrophage Polarization: Different Gene Signatures in M1(LPS+) vs. Classically and M2(LPS-) vs. Alternatively Activated Macrophages. Front Immunol, 10, 1084. [PubMed: 31178859]

Patel KS, Kejriwal S, Sun MM, Thammachantha S, Duong C, Chan A, Cherian N, Romiyo P, Gordon LK, Yong W, Wadehra M & Yang I 2020. Identification of epithelial membrane protein 2 (EMP2) as a molecular marker and correlate for angiogenesis in meningioma. J Neurooncol, 147, 15–24. [PubMed: 31981014]

Robertson SA, Care AS & Moldenhauer LM 2018. Regulatory T cells in embryo implantation and the immune response to pregnancy. The Journal of Clinical Investigation, 128, 4224–4235. [PubMed: 30272581]

Seshadri S & Sunkara SK 2014. Natural killer cells in female infertility and recurrent miscarriage: a systematic review and meta-analysis. Hum Reprod Update, 20, 429–38. [PubMed: 24285824]

Sojka DK, Yang L, Plougastel-Douglas B, Higuchi DA, Croy BA & Yokoyama WM 2018. Cutting Edge: Local Proliferation of Uterine Tissue-Resident NK Cells during Decidualization in Mice. J Immunol, 201, 2551–2556. [PubMed: 30275046]

Sojka DK, Yang L & Yokoyama WM 2019. Uterine Natural Killer Cells. Front Immunol, 10, 960. [PubMed: 31118936]

Sun MM, Chan AM, Law SM, Duarte S, Diaz-Aguilar D, Wadehra M & Gordon LK 2019. Epithelial Membrane Protein-2 (EMP2) Antibody Blockade Reduces Corneal Neovascularization in an In Vivo Model. Invest Ophthalmol Vis Sci, 60, 245–254. [PubMed: 30646013]

Svensson-Arvelund J, Mehta RB, Lindau R, Mirrasekhian E, Rodriguez-Martinez H, Berg G, Lash GE, Jenmalm MC & Ernerudh J 2015. The Human Fetal Placenta Promotes Tolerance against the Semiallogeneic Fetus by Inducing Regulatory T Cells and Homeostatic M2 Macrophages. The Journal of Immunology, 194, 1534–1544. [PubMed: 25560409]

Tirado-González I, González IT, Barrientos G, Freitag N, Otto T, Thijssen VL, Moschansky P, Von Kwiatkowski P, Klapp BF, Winterhager E, Bauersachs S & Blois SM 2012. Uterine NK cells are critical in shaping DC immunogenic functions compatible with pregnancy progression. PLoS One, 7, e46755. [PubMed: 23056436]

Toth B, Zhu L, Karakizlis H, Weimer R, Morath C, Opelz G, Kuon RJ & Daniel V 2020. NK cell subsets in idiopathic recurrent miscarriage and renal transplant patients. J Reprod Immunol, 138, 103098. [PubMed: 32045760]

Tsuda S, Nakashima A, Shima T & Saito S 2019. New Paradigm in the Role of Regulatory T Cells During Pregnancy. Front Immunol, 10, 573. [PubMed: 30972068]

Wadehra M, Dayal M, Mainigi M, Ord T, Iyer R, Braun J & Williams CJ 2006. Knockdown of the tetraspan protein epithelial membrane protein-2 inhibits implantation in the mouse. Dev Biol, 292, 430–41. [PubMed: 16487956]

Wadehra M, Su H, Gordon LK, Goodglick L & Braun J 2003. The tetraspan protein EMP2 increases surface expression of class I major histocompatibility complex proteins and susceptibility to CTL-mediated cell death. Clin Immunol, 107, 129–36. [PubMed: 12763482]

Williams CJ, Chu A, Jefferson WN, Casero D, Sudhakar D, Khurana N, Hogue CP, Aryasomayajula C, Patel P, Sullivan P, Padilla-Banks E, Mohandessi S, Janzen C & Wadehra M 2017. Epithelial membrane protein 2 (EMP2) deficiency alters placental angiogenesis, mimicking features of human placental insufficiency. J Pathol, 242, 246–259. [PubMed: 28295343]

Williams PJ, Searle RF, Robson SC, Innes BA & Bulmer JN 2009. Decidual leucocyte populations in early to late gestation normal human pregnancy. J Reprod Immunol, 82, 24–31. [PubMed: 19732959]

Wu Y, Sarkissyan M, Elshimali Y & Vadgama JV 2013. Triple negative breast tumors in African-American and Hispanic/Latina women are high in CD44+, low in CD24+, and have loss of PTEN. PLoS One, 8, e78259. [PubMed: 24167614]

Yao Y, Xu X-H & Jin L 2019. Macrophage Polarization in Physiological and Pathological Pregnancy. Frontiers in Immunology, 10.

Zhang JH, Yamada AT & Croy BA 2009. DBA-lectin reactivity defines natural killer cells that have homed to mouse decidua. Placenta, 30, 968–73. [PubMed: 19765824]

Zhang YH, He M, Wang Y & Liao AH 2017. Modulators of the Balance between M1 and M2 Macrophages during Pregnancy. Front Immunol, 8, 120. [PubMed: 28232836]

Highlights

- The overall percentage of CD45+ cells is increased in *Emp2* KO compared to WT mice in the decidua and placenta.
- uNK cells were increased in the placental beds of *Emp2* KO animals.
- Double-knock out of *Emp2* and NK cells did not alter individual pup birthweight, but it did significantly reduce total litter weight and size by ~50%.
- In conclusion, *Emp2* appears to regulate uNK and macrophage cell populations in pregnancy.

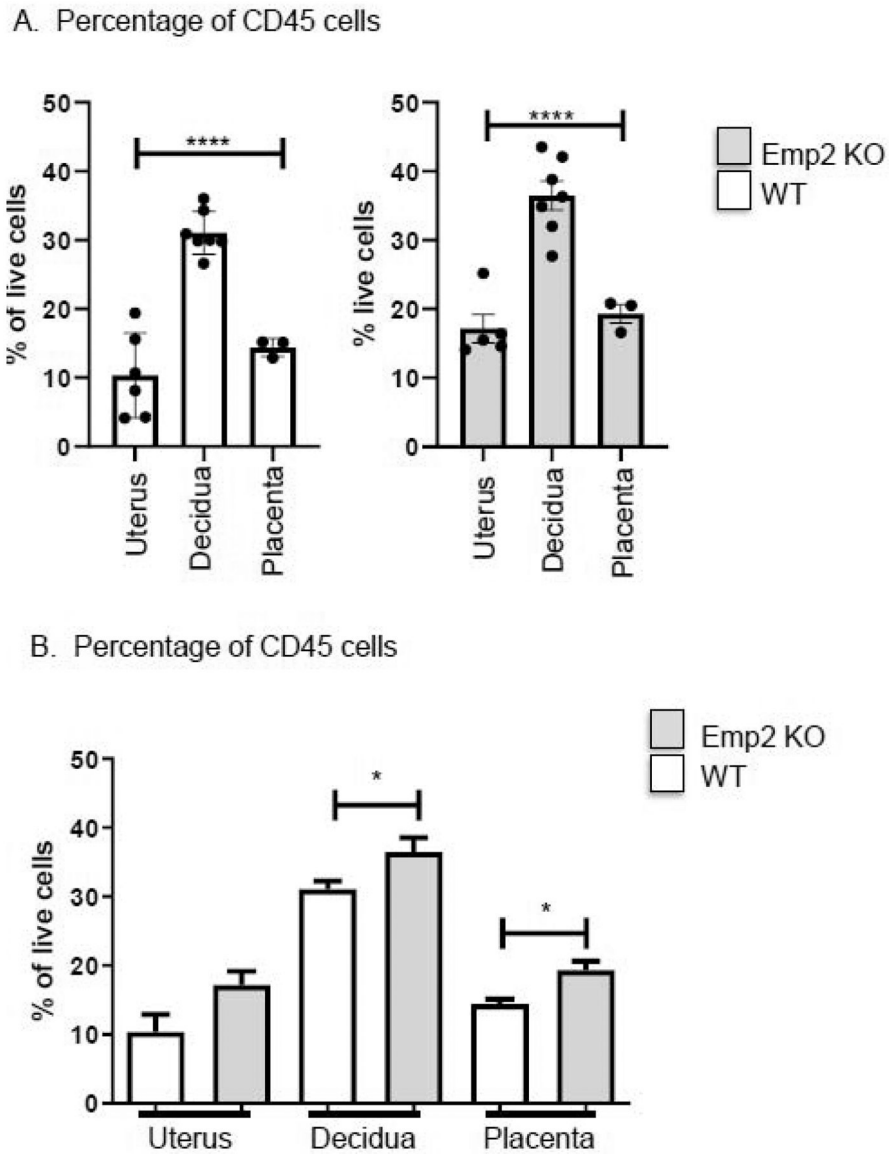

Figure 1: *Emp2* KO mice have an increased percentage of CD45+ cells in the decidua and placenta at GD12.5 compared to WT mice.

(A) Graphs depict the percentage of CD45+ cells of all live cells isolated from the decidua, placenta, and uterus in WT (open bars) and *Emp2* KO (grey bars) mice. In both WT and *Emp2* KO mice, significant differences exist among the three locations (*** indicates $p<0.0001$ using ANOVA). (B) There is a significant increase in the percentage of CD45+ cells in the decidua in *Emp2* KO compared to WT mice (WT: 31.07±1.18%, *Emp2* KO: 36.47±2.10%; $p=0.045$ by Student's t-test, n=7/group). There is also a significant increase in the percentage of CD45+ cells in the placenta in *Emp2* KO compared to WT mice (WT: 14.40±0.75%, *Emp2* KO: 19.30±1.35%; $p=0.034$ by Student's t-test, n=3/group). There was no difference between the percentages of CD45+ cells in the uterus. Data are represented as mean ± SEM and show the compiled results from 3 independent experiments using pooled samples from at least 3 mice/group.

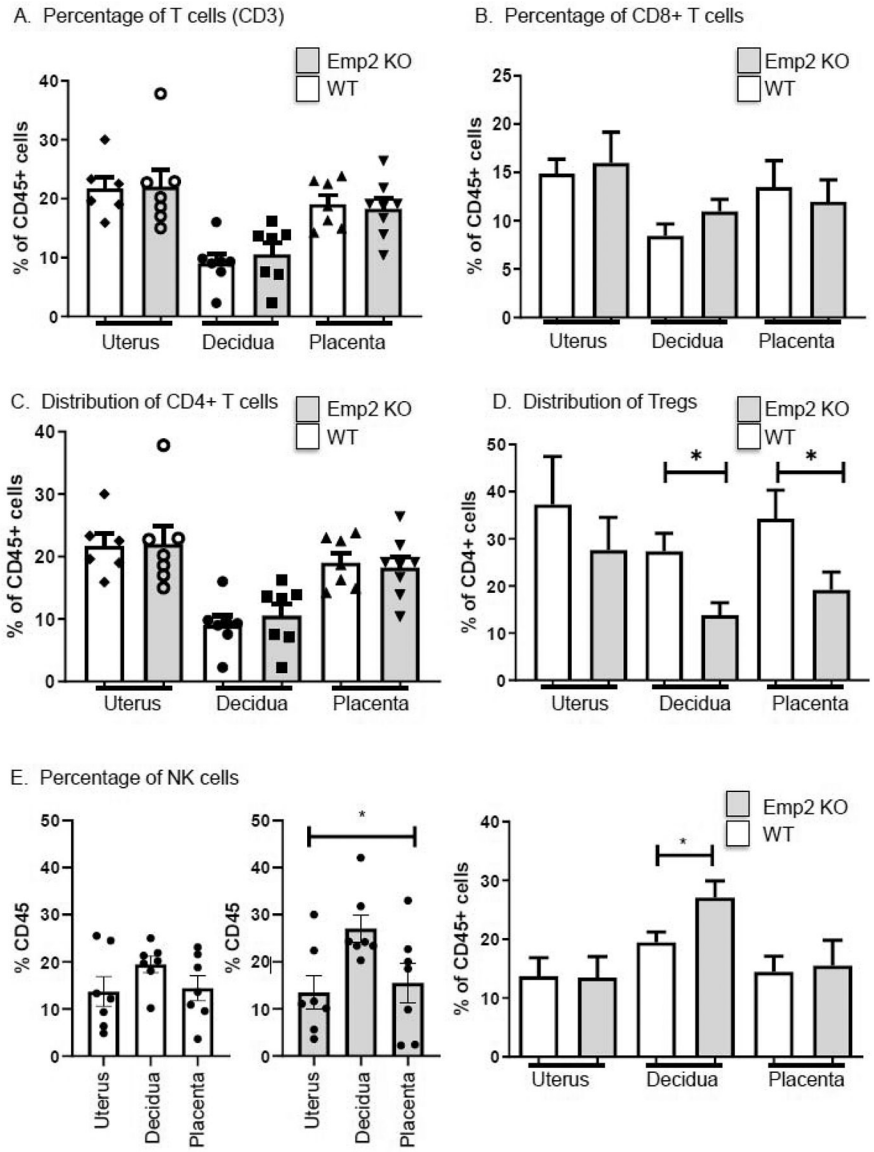

Figure 2: *Emp2* KO mice have an increased percentage of NK cells and decreased percentage of T regulatory cells in the decidua at GD12.5 compared to WT mice

(A) Graphs depict the percentage of T (CD3+) cells of CD45+ cells isolated from the decidua, placenta, and uterus in WT (open bars) and *Emp2* KO (grey bars) mice. CD3+ T cells do not display differences in percentage of CD45+ cells across the tissue types in WT or *Emp2* KO mice. Moreover, there are no differences between WT and *Emp2* KO mice CD3+ T-cell percentages in the uterus, decidua or placenta (n=5–6 samples/group). Stratification of CD3+ cells into CD4− (B) and CD4+ (C) reveal no significant differences in percentages between the WT and *Emp2* KO uterus, decidua, and placenta. (D) Usage of CD24 and folate receptor 4 (FR4) antibodies further subdivided CD4+ populations among the different sites. T regs showed significant downregulation in the *Emp2* KO decidua and placenta compared to the WT. (E) Graphs depict the percentage of NK cells relative to CD45+ cells isolated from the decidua, placenta, and uterus in WT (open bars) and *Emp2* KO (grey bars) mice (n=7 samples/group/tissue). No differences in the percentage

of NK cells across the tissue types occurred in WT mice, but *Emp2* KO mice showed significant differences among the different locations tested (*p=0.02, ANOVA). Moreover, the percentage of NK cells in the decidua increased in the *Emp2* KO group compared to the WT group (*p=0.04, Mann Whitney). Data are presented as the mean and SEM and show the compiled results from 3 independent experiments using pooled samples from at least 3 mice/group.

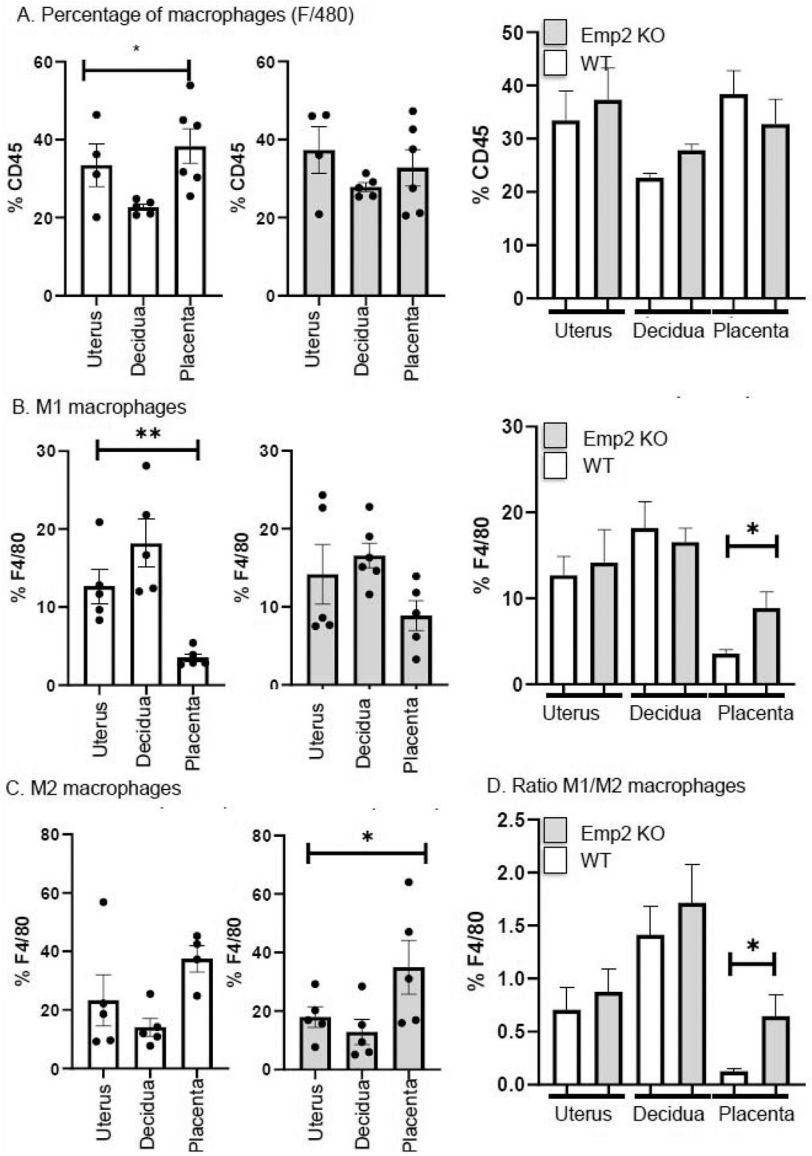

Figure 3: *Emp2* KO mice have an increased percentage of M1 macrophages in the placenta at GD12.5 compared to WT mice

(A) Graphs depict the percentage of macrophages (F4/80+) cells of CD45+ cells isolated from the decidua, placenta, and uterus in WT (open bars) and *Emp2* KO (grey bars) mice. Macrophages represent the largest percentage of immune cells in all tissues, and do display differences in the percentage of CD45+ cells across the tissue types in WT (*p=0.03, ANOVA), but not *Emp2* KO mice. However, there are no differences between WT and *Emp2* KO mouse macrophage percentages in the uterus, decidua or placenta (n=4–6 samples/group). B) Graphs depict the percentage of M1 macrophages (MHCII+) from the total F4/80+ cells isolated from the decidua, placenta, and uterus in WT (open bars) and *Emp2* KO (grey bars) mice. WT mice display significant differences in the percentage of MHCII+ cells across the tissue types (**p=0.005, ANOVA), with the largest percentage of M1 macrophages present in the decidua. *Emp2* KO mice do not display significant differences in the M1 macrophage percentage in the various tissues. However, there is an

increased percentage of M1 macrophages in *Emp2* KO mice in the placenta compared to WT mice (*p=0.03, Student's t test). C) Graphs depict the percentage of M2 macrophages (CD206+) from the F4/80+ cells isolated from the decidua, placenta, and uterus in WT (open bars) and *Emp2* KO (grey bars) mice (n=4–5 samples/group). *Emp2* KO mice display differences in the percentage of CD206+ macrophages across the tissue types (*p=0.04, ANOVA), with the largest percentage of M2 macrophages present in the placenta. WT mice do not display significant differences in the M2 macrophage percentage across the various tissues. D) However, there is an increased M1/M2 macrophage ratio in *Emp2* KO mice in the placenta compared to WT mice (*p=0.03, Student's t test). Data are represented as mean ± SEM and show the compiled results from 3 independent experiments using pooled samples from at least 3 mice/group.

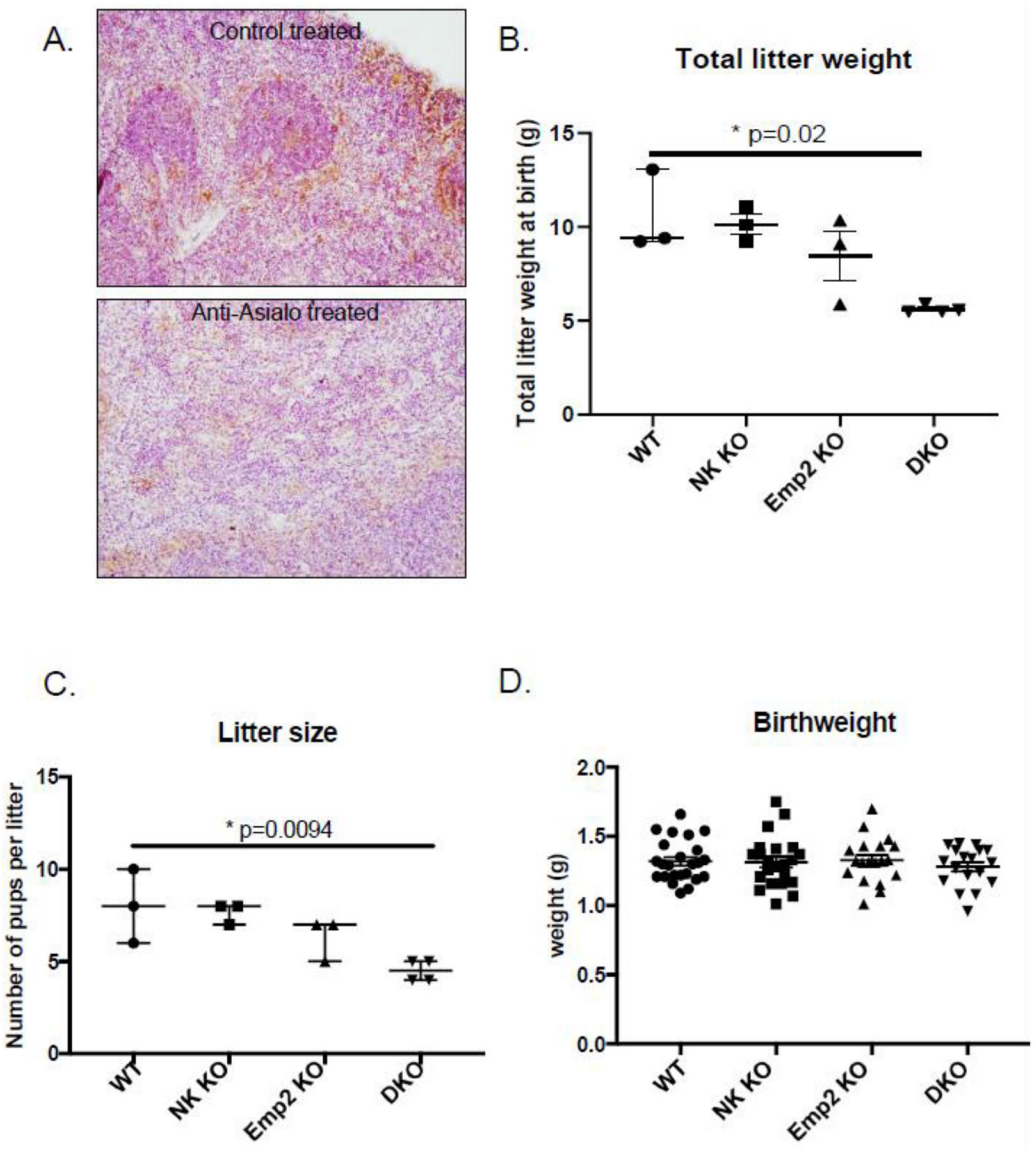

Figure 4: NK cell depletion in *Emp2* KO mice leads to decreased litter sizes and total litter birthweight.

A) Semi-quantitative determination for NK cell depletion in WT and Emp2 KO mice using anti-asialo GM1 vs control IgG injections. Representative images taken at 400X magnification of the spleen taken from *Emp2* KO mice treated with control non-targeted IgG antibody (top) or anti-asialo GM1 injections (bottom) showing NK cell (NKp46 visualized using DAB staining) depletion in the anti-asialo GM1-treated mice. B) Graph depicts total litter weight in grams in WT (WT+sham), NK KO (WT+ anti-asialo GM1), *Emp2* KO (*Emp2* KO + sham), and *Emp2* DKO (*Emp2* KO + anti-asialo GM1) groups. Data is presented as the median and quartile range indicated. There is a significant reduction in total litter weight in the *Emp2* DKO groups (median: 5.538g; quartile range: 5.495–5.828, n=4 litters) compared to WT (median 9.41; interquartile range: 9.23–13.05; n=3 litters), NK KO (median: 10.12; interquartile range: 9.22–11.1; n=3 litters) and *Emp2* groups (median: 9.08; interquartile range: 5.87–10.35; n=3 litters) (p=0.02 by Kruskal-Wallis testing). C)

Graph depicts total litter size in WT (WT+sham), NK KO (WT+ anti-asialo GM1), *Emp2* KO (*Emp2* KO + sham), and *Emp2* DKO (*Emp2* KO + anti-asialo GM1) groups. Data are represented as median and interquartile range. The reduction in total litter weight is attributable to decreased litter size in the *Emp2* DKO group (median: 4; interquartile range: 4–5; n=4 litters), compared to WT (median: 8; interquartile range: 6–10; n=3 litters), NK KO (median 8; interquartile range: 7–8; n=3 litters) and *Emp2* KO groups (median: 7; interquartile range: 5–7; n=3 litters) (p=0.0094 by Kruskal-Wallis testing). D) Graph depicts pup birthweights in grams in WT (WT+sham), NK KO (WT+ anti-asialo GM1), *Emp2* KO (*Emp2* KO + sham), and *Emp2* DKO (*Emp2* KO + anti-asialo GM1) groups. Data are represented as mean and SEM. There were no differences in the individual pup birthweights between the WT (1.32±0.03; n=24 pups), NK KO (1.315±0.04; n=22 pups), *Emp2* KO (median: 1.33±0.04; n=19 pups), and *Emp2* DKO groups (1.28±0.03; n=18 pups) (p=0.86 by Kruskal-Wallis testing).

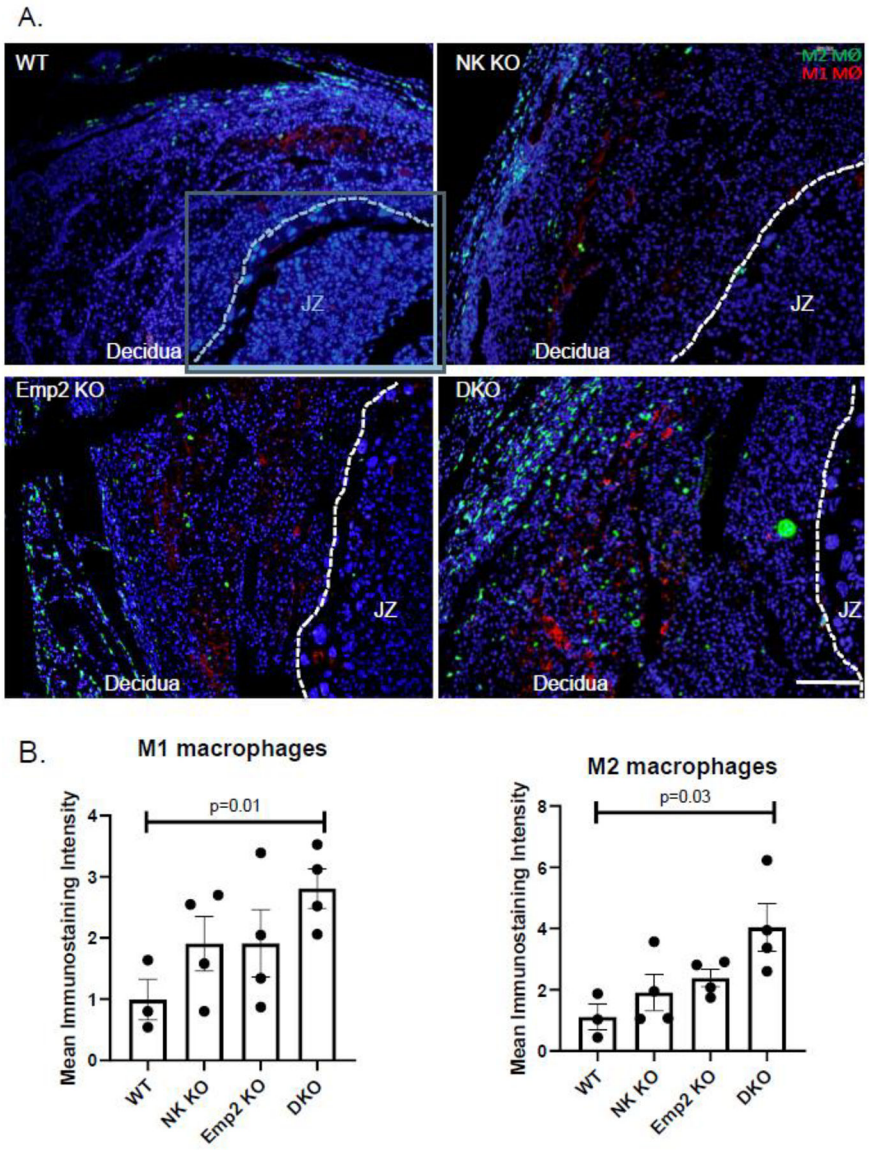

Figure 5. NK cell depletion in *Emp2* KO mice leads to increased macrophage recruitment.

A. Representative images taken at 100X magnification of the placenta taken from WT or *Emp2* KO mice treated with control non-targeted IgG antibody or anti-asialo GM1 injections. Sections were stained for M1 macrophages or M2 macrophages using anti-iNOS (Texas Red) or anti-CD206 (FITC) antibodies, respectively, and nuclei were counterstained using DAPI. The division between the junctional zone (JZ) and decidua was demarcated using the nuclei of trophoblast giant cells. Merged images are shown. Scale bar = 200 μm. B. Semi-quantitative determination of the mean staining intensity of M1 (Texas-Red) and M2 (FITC) macrophages in WT and *Emp2* KO mice treated with anti-asialo GM1 vs control IgG injections. Graph represents the mean pixel count for each color ± SEM from 3 independent experiments using isolated decidua from at least 3 mice/group. A one way ANOVA was used to compare the means between groups.